

Methods

To study the morphology of streamers and leaders in an 0.8 m rod-to-rod air gap between hemispherical and conical electrodes, the LABELLEC high-voltage laboratory in Terrassa, Spain was used. Using a Phantom TMX 6410 high-speed camera allowed us to study the discharge at 750 kfps. The experimental setup, data analysis pipeline and the approach are covered in this chapter.

Experimental setup

A schematic of the experimental setup can be seen in Figure 0.1. The high-voltage impulses were generated using a Marx generator capable of producing up to 1 MV, specifically with a Haefely impulse generator, configured to deliver a switching impulse waveform of 150/2000 μ s. A Marx generator charges multiple capacitors in parallel to a moderate voltage (100 kV for the used generator) and then, via triggered spark gaps, reconnects them in series to produce a high-voltage impulse. The Marx generator is connected to front resistors which shape the impulse waveform. The front resistors send the voltage pulse to a voltage divider, which divides a fraction of the generator voltage, delivering a replica of the voltage to an oscilloscope for measuring the waveform. The oscilloscope was set to measure at 5 MS/s. Current at the grounded electrode was measured with two transformers: A Pearson Model 110A and a custom ferrite-core transformer developed by M. Arcanjo, tested here and intended for field measurements of upward streamers and leaders [1]. Both outputs were routed, via shielded cables, to the same oscilloscope. The impulse was applied to a 0.8 m (stainless steel) rod-to-rod gap, a length chosen as no breakdown occurred at a gap of 1 m under negative polarity at the maximum output voltage. Insulator rings are present to prevent accidental flashover when the Marx generator applies its impulse.

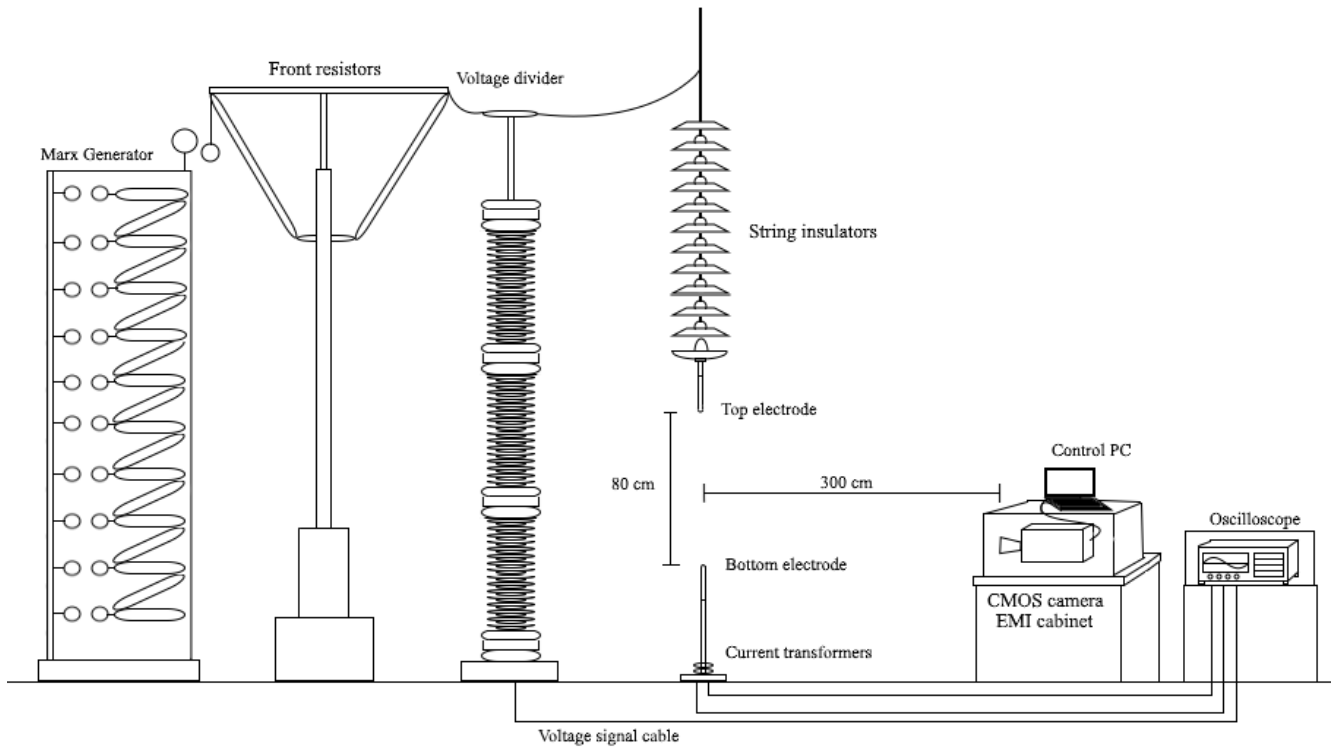


Figure 0.1: Schematic of the experimental setup. A switching impulse (150/2000 μ s) is applied across a 0.8 m stainless-steel rod-to-rod gap with a Marx generator and front resistors, connected to a voltage divider which samples the waveform to an oscilloscope. Current transformers monitor currents at the grounded electrode. A Phantom TMX 6410 high-speed CMOS camera records at 752 kfps from within an EMI-shielded cabinet.

A Phantom TMX 6410 high-speed monochrome camera fitted with a 50 mm f/1.4 lens was used for the optical diagnostics. The camera recorded at 752066 fps in 128 x 512 or 128 x 640 pixels, depending on the session. The image size was the limiting factor on the maximum fps on the camera. A smaller pixel width enabled higher frame rates but risked missing events outside of the frame. A decision was made to use the 128 pixel width, at 750 kfps (kilofps) to map the discharge with sufficient temporal and spatial resolution. The fps resulted in a frame interval of 1.33 μ s and an exposure time of 1.06 μ s per frame. To ensure alignment of the video and oscilloscope measurements, .cine files (files of the Phantom Camera Control (PCC)) were shortened so that the Marx generators light-flash (due to the spark between capacitor sphere gaps) appeared at the start of the sequence; in later recordings, a ten-frame pre-flash buffer was used to improved noise estimation. The camera, power source and control electronics were housed inside an electro magnetic interference (EMI) shielded cabinet situated 300 cm from the spark gap. Two trigger schemes were tested and used. First, image-based auto-trigger was implemented, where detecting optical intensity changes resulted in the start of the recording. Second, an external trigger mode based on a threshold crossing of the voltage signal. Both methods have its advantages and disadvantages. As the image based trigger is easy to setup, but did not consistently trigger in cases where a discharge did not reach breakdown. Although the voltage based trigger did consistently trigger correctly, there was a risk of EMI corrupting the trigger signal or an induce voltage spikes due to the spark that can damage the camera's hardware.

All tests were performed with a four-channel oscilloscope logging voltage and current, while the high-speed video was recorded separately. Room conditions varied between 18°C and 21°C with 51% humidity at approximately 1 atm. Discharges were spaced by at least two minutes to allow residual ionization to decay fully. For each electrode geometry, shown in Figure 0.2; sharp conical tips (20 cm total length, 20 mm width, 6 cm cone, 1 mm tip) and blunt hemispherical tips (20 cm long, 20 mm wide, 10 mm tip height), a minimum of twenty valid shots were acquired for each polarity. Input voltages were chosen by iteratively changing the Marx output until a 50% breakdown probability was reached for each configuration. Because breakdown in long air gaps does not happen at exactly the same voltage every time, a 'characteristic' voltage is defined by finding the level where half of our trials break down and half do not (often called U_{50}). This 50% breakdown probability reduces random effects, so that the results become reproducible and comparable across different setups. It's also the standard way to report breakdown voltages in most high-voltage testing protocols [2,5].

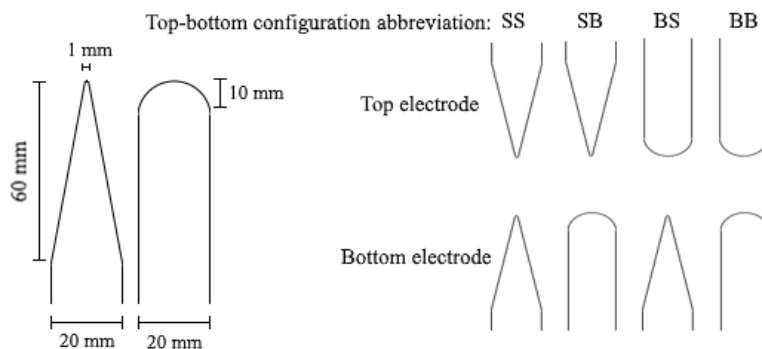


Figure 0.2: Schematic of the used electrodes and configuration abbreviations, derived from the top-bottom electrode position and shapes: sharp (S) and blunt (B).

Data quality was monitored from a control room. Unfortunately, measurements in which the camera's current-session reference (CSR) was configured incorrectly were discarded. A CSR closes the camera's internal shutter and resets the black point of every pixel to improve quality; essentially a dark-frame calibration step. Despite numerous discarded recordings, each geometry and polarity has sufficient valid discharges to support meaningful analysis of streamer zones and leader channels.

Data processing pipeline

An image-processing pipeline was used to extract results from all recordings, implemented fully in MATLAB. The pipeline start by loading raw PCC .cine files into MATLAB using a Vision Research provided code, called 'Phantom SDK' (version 3.11.11.806), from which the unchanged image pixel values can be obtained. Being able to use the cine files is advantageous, as the files do not have to be converted to another file type, reducing quality or pixel depth.

Before loading the .cine video files into MATLAB, the recordings were edited in the PCC software to have a gain of 5000, gamma correction at 4.5, and a flare setting of 0.25%, as shown in Figure 0.3. Adjusting the parameters controls how the sensor data is mapped into pixel values. The gain multiplies each pixel's raw signal, amplifying both signal and noise. Dim features now become more visible at the expense of increased noise. The gamma correction applies a nonlinear tone curve so that mid-tone details are shown better, without saturating the already bright pixels. The flare (or 'pedestal') adds a small constant offset to each pixel, improving thresholding in further processing. These parameters provided a sufficient range to capture both faint streamer details and bright leader channels while keeping noise at an acceptable level and not losing detail due to saturation.

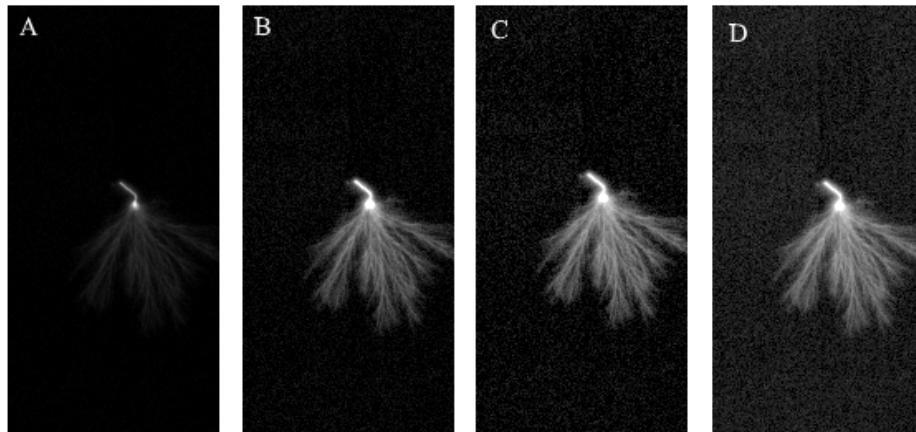


Figure 0.3: Comparison of PCC image-processing parameters on a single discharge frame. (a) Default settings. (b) Gain increased to 5000. (c) Gamma corrected to 4.5. (d) Flare set to 0.25%.

For each shot, the pipeline began by loading every frame and computing pixel intensities to rank frames by brightness. The ten darkest frames, assumed free of discharges, were averaged to form a mean background, and their pixel dependent standard deviation was used to generate a minimal limit for noise. Every subsequent frame had its background subtracted. Pixels below a noise floor or with negative value, were set to zero. Depending on the intensity of each pixel, each frame was then binarized. Further morphological closing with eliminated small gaps and morphological opening reduced the remaining loose pixels in the frame.

Frame timing was aligned by assigning zero microseconds to the first frame with a pixel value exceeding 50% of the maximum pixel value (12-bit depth = 4095). This point corresponded to the initial bright flash from the Marx generator and the start of the ramp-up of the voltage. By dividing over the fps, the time between frames was determined and assigned to each frame. After aligning the frame times, the voltage and current traces were also aligned to each frame. Discharge phases were identified automatically: The first frame containing non-zero processed pixels after the Marx generator flash marked the first corona phase. Final breakdown was determined by choosing the frame with the highest value of the sum of all pixels, above a threshold corresponding to a 90% fully saturated screen. Within the determination of the flash frame, the electrodes are visible, as light reflects of the steel surfaces, shown in Figure 0.4. The

same figure also shows how with the use of the pixel intensity of the reflected light, an outline of the electrode is drawn. The detection and outlining of the electrode works for each video, but small changes to the size had to be made for videos where the electrodes did not appear as bright.

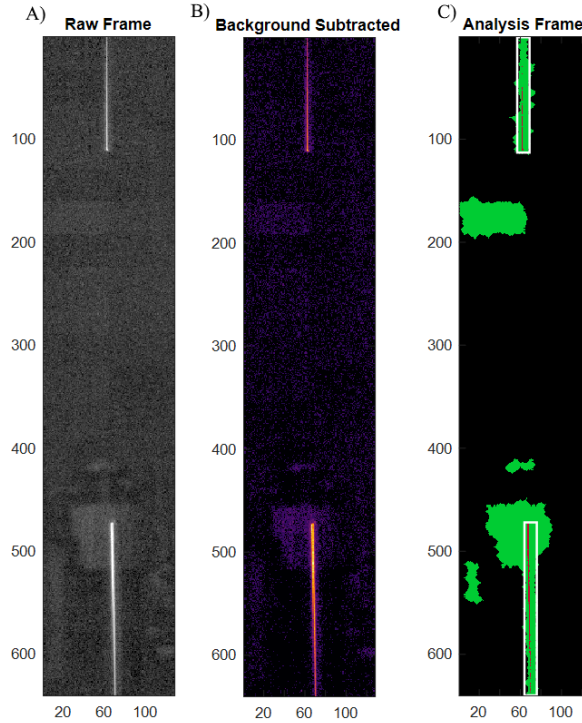


Figure 0.4: Image-processing steps for a single discharge frame showing the Marx generator flash illuminating the test chamber. (a) Raw frame. (b) Background-subtracted false-color frame. (c) Binarized frame with electrode regions detected and outlined.

Streamers and leaders are separated by their intensity, after background subtraction, as shown in Figure 0.5 A-C. By looking at histograms of the intensities of certain frames, a threshold for leaders was put at 50% of the maximum intensity of all frames. Taking a threshold for each frame separately would result in the detection of streamers and leaders in frames where no activity was present. From the detected streamers and leaders in the binary masks, high-intensity starting points were determined within an electrode region of interest. Detection of a starting point in the electrode region confirmed these as streamer bursts, rather than the streamers connected to leader tips. The detection of leader bodies outside of the electrode region were labeled as leader tips. Large stems could be labeled as a leader tip, but are at most a few cm long and of a short duration, making a distinction with leaders that show constant growth. All remaining pixels were labeled as streamers.

For leaders the tip coordinates are saved, as shown in Figure 0.5 D. To characterize the streamer, a decision was made to fit a cone on the streamer zone. The approach resembles the shape taken by models of Becerra and Cooray [3] and the typical shape seen in streak images of long gap discharges [4]. Cone fitting is performed by the covering of the streamer zone within an arc, surrounding the leader tip as a center point. Streamer-fit pixels are limited to those lying 'in front' of the leader tip by testing the sign of the dot-product between two vectors: First, a unit vector pointing outward from the nearest electrode toward the tip is defined. Then, for each candidate pixel, the vector from the leader tip to that pixel is computed. Only pixels whose dot-product with the outward unit vector is positive, meaning they lie in the half space away from the electrode, are retained. This is done to exclude pixels belonging to the leader channel from the fit. In Figure 0.5 E, an example of the fitted arc covering the entire streamer

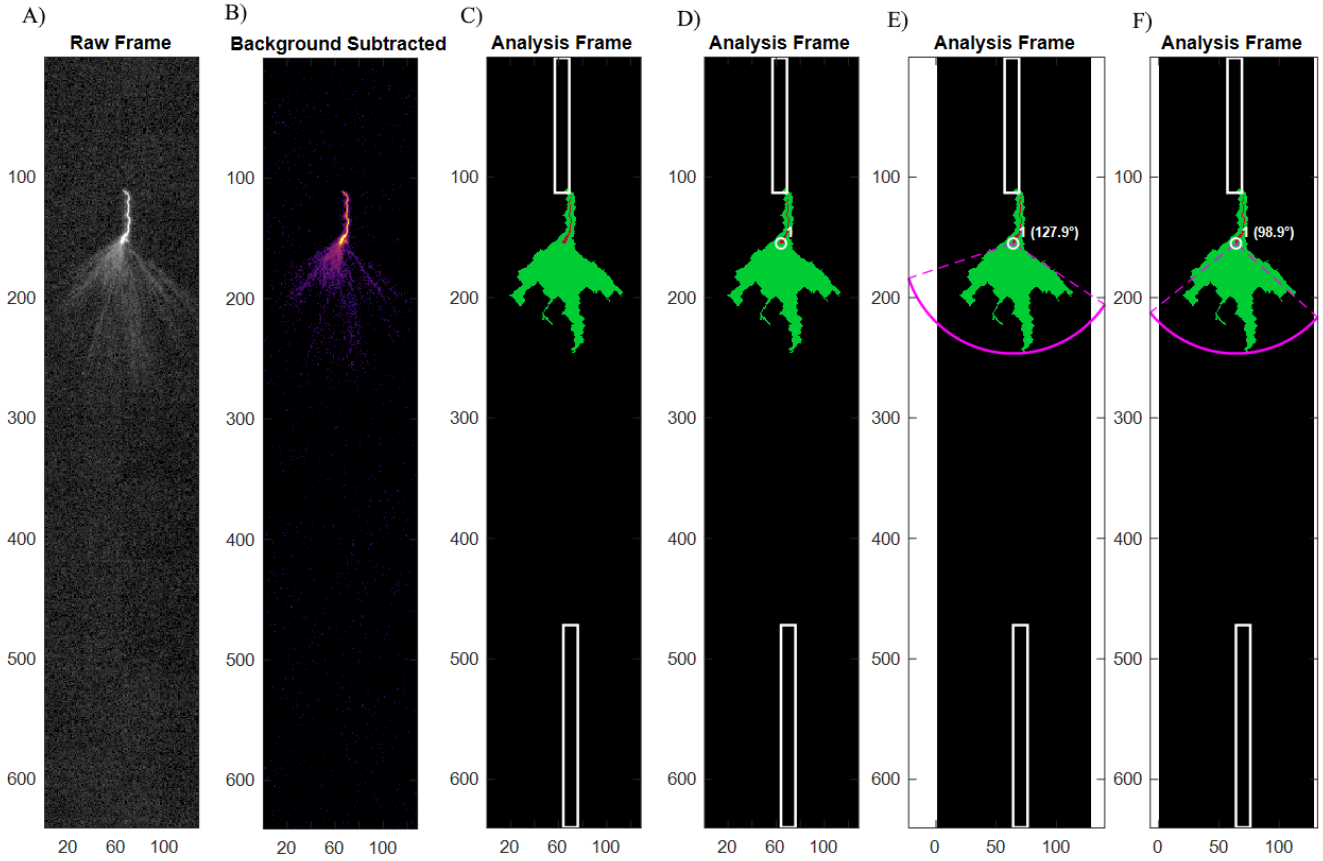


Figure 0.5: Stepwise image-processing pipeline for extracting data from a single discharge frame. (A) Raw frame showing a streamer corona. (B) Background subtraction and false-color scaling. (C) Binarized analysis frame with electrode regions and distinction between the leader and streamer body. (D) Same binary frame with the detected leader tip marked. (E) Initial overestimated arc fit. (F) Improved arc fit applied to the main 90% of streamer pixels, for a more realistic opening angle.

region is shown, but the computed opening angle is overestimated. By selecting the leader tip as the arc's center, defined as the furthest pixel from the electrode, the fit must include streamer branches that begin spreading before the leader tip, increasing the cone angle. To address the issue, Figure 0.5 F shows an arc fitting approach that uses approximately 95% of the streamer pixels, omitting the cluster close to the tip. This narrower selection yields a more realistic opening angle, though a small fraction of the outer streamer body lies outside the arc. This method yields, for each streamer zone, the cone opening angle and the streamer burst's length and (arc) width. The code also checks the distance to each electrode and whether the region connects back to the top or bottom electrode and labels it accordingly as a streamer or counter-streamer.

Limitations

While the cone-fitting approach works for capturing simple streamer morphology, the approach simplifies the often irregular shape of streamer coronas. The assumption of a perfect circular arc neglects finer details and any asymmetries in the branches. Furthermore, in the counter-streamer direction (i.e., from the bottom electrode), the absence of a true leader channel combined with bright streamer emissions sometimes triggers detection of a false leader tip. However, because we record and label the connection of each event's electrode connected, we can identify and exclude these outliers during post-processing. The current algorithm also merges multiple streamer zones into a single cone when they emerge from

one leader, since it identifies only a single leader tip point per connected region. As a result, discharges exhibiting two or more distinct streamer bursts attached to the same leader are incorrectly represented in the statistics. Examples of the limitations are shown in Chapter ??.

Background subtraction is needed to remove noise, but also introduces uncertainty. Taking an average of the darkest frames to estimate and remove the static background works, but can also result in removing faint streamers. Furthermore, pixels falling outside the camera's field of view are excluded from the analysis. The fitting approach allows the ideal arc to extend beyond the image borders, however, the streamer metrics (length, width, area) will be an underestimation of the actual dimensions. By manually comparing fitted cones to the visible streamer bodies, relative length errors as large as 60%, and area errors even higher have been found. These values have been found under the assumption that the streamer should fully occupy the fitted arc.

Experimental outline

Four electrode configurations were tested, combining sharp and blunt electrodes at the top and bottom. In the results, each configuration is labeled by 'top-bottom-polarity.' For example, a sharp top electrode, a blunt bottom electrode, and positive polarity is denoted 'sharp-blunt-positive' (SBP), referring back to the abbreviation shown in Figure 0.2. Each experiment involved capturing high-speed video alongside synchronized voltage and current waveforms for both polarities. By matching frame timestamps to the oscilloscope records, the complete discharge sequence was reconstructed.

For each geometry and polarity, the Marx output was adjusted to reach U_{50} : the voltage at which half of the impulses resulted in a discharge, ensuring statistically accurate comparison in different conditions. Around 20-30 impulses were fired, and the presence or absence of breakdown was noted. The voltage peak of the waveform data were identified and collected. The mean value was then determined to find U_{50} and compared for the polarities and configurations.

First corona timing was determined by reviewing each high-speed video to locate the first frame in which a faint, localized inception cloud or streamer appeared on the electrode. The frame index was converted to a delay relative to the Marx generator flash at $t = 0 \mu\text{s}$). Full breakdown timing was then extracted by identifying the frame where the discharge saturated all pixels. The time of that frame is recorded, and the corresponding drop in voltage on the oscilloscope trace was used to confirm and refine the breakdown timing. The process was repeated for each shot, resulting in configuration dependent statistics on inception and breakdown timing.

From the high-speed videos of positive discharges, sequences exhibiting clear leader propagation show clear leader growth over time, meaning that the leader velocity can be derived. The leader tip was marked in each frame, and its pixel coordinates were converted to centimeter using a pixel to centimeter conversion. Plotting displacement over time and fitting a straight line resulted in an average propagation speed for each leader, the combination of all leader velocities, for each configuration was then averaged to produce the average velocities.

Each frame has its background subtracted and is binarized to isolate the streamer corona. The cone-fitting algorithm then fits 90% of streamer pixels, resulting in an opening angle, radial streamer length, and arc width for each frame. As the cone fitting approach has not shown very accurate results, frame-to-frame variability was deemed to be too high, so data is smoothed to allow the study of underlying trends. Although the presented values are an approximation, the resulting time-series can still be studied.

References

- [1] M. Arcanjo, J. Montanya, M. Urbani, and V. Lorenzo. Measuring low-current discharges from grounded rods under high background electric fields. *Electric Power Systems Research*, 217:109139, 2023.
- [2] Asociacion Espanola de Normalizacion (UNE) / IEC. Une-en iec 61400-24:2019 - aerogeneradores. parte 24: Proteccion contra el rayo. National adoption of international standard, Asociacion Espanola de Normalizacion (UNE) / IEC, Bristol, 2019. Ratified by UNE June 1, 2020; identical to IEC 61400-24:2019.
- [3] M. Becerra and V. Cooray. A self-consistent upward leader propagation model. *Journal of Physics D: Applied Physics*, 39(16):3708, aug 2006.
- [4] I. Gallimberti. The mechanism of the long spark formation. *Journal de Physique Colloques*, 40(C7):C7–193–C7–250, July 1979. XIVe Conference Internationale sur les Pheomenes d’Ionisation dans les Gaz / XIVth International Conference on Phenomena in Ionized Gases.
- [5] International Electrotechnical Commission. Iec 60060-1:2025 - high-voltage test techniques - part 1: General terminology and test requirements. International standard, International Electrotechnical Commission, Geneva, 2025. 4th edition, replaces IEC 60060-1:2010; published April-June 2025.
- [6] Vision Research / Phantom High-Speed. Spectral response curve of the phantom tmx 6410. Online datasheet image, 2025. Accessed July 2025; available at <https://www.phantomhighspeed.com/products/cameras/tmx/64106273759322001>.
- [7] Y. Xie, H. He, C. Wu, and J. He. An experimental and numerical study of leader development in rod-rod gaps under positive switching impulse voltage. *The European Physical Journal Applied Physics*, 64(1):10802, 2013.

A Appendix

A.1 QQ-plot streamer opening angles

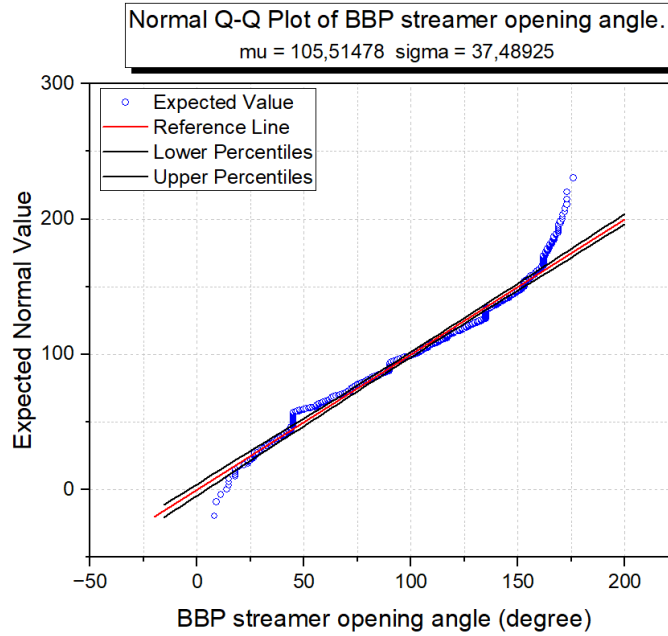


Figure A.1: QQ plot for the BBP configuration, indicating heavy tails. No normal distribution can be obtained from the data.

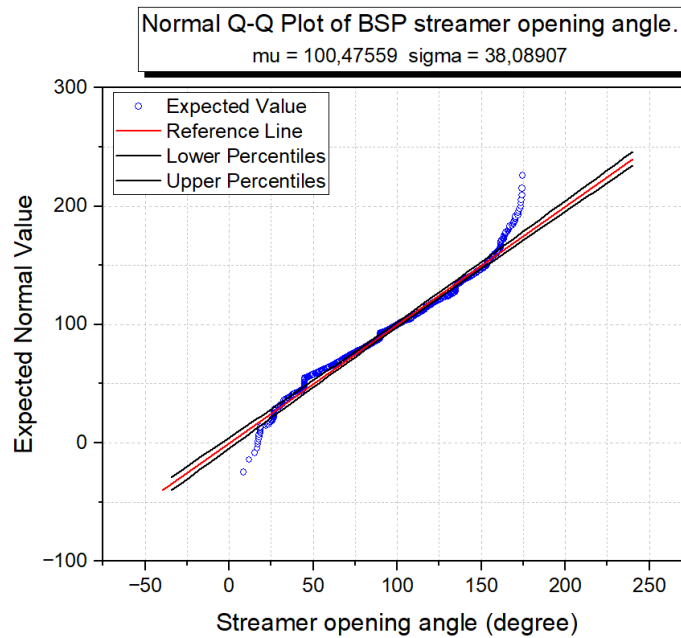


Figure A.2: QQ plot for the BSP configuration, indicating heavy tails. No normal distribution can be obtained from the data.

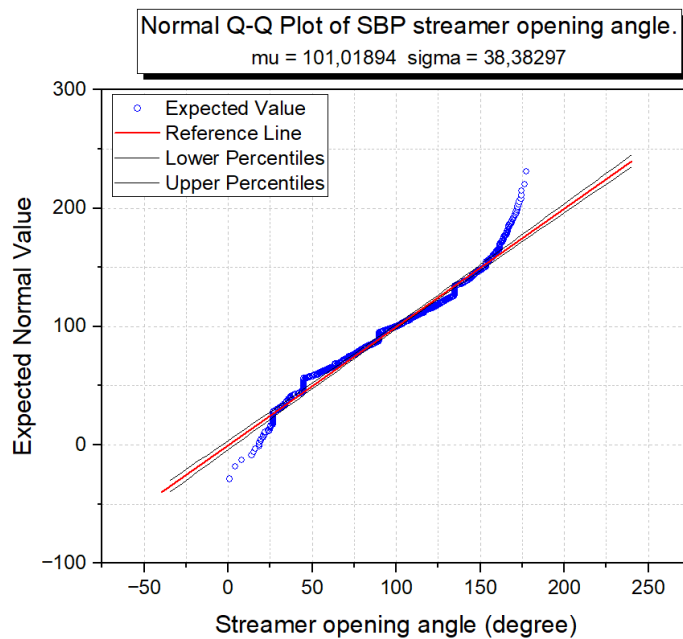


Figure A.3: QQ plot for the SBP configuration, indicating heavy tails. No normal distribution can be obtained from the data.

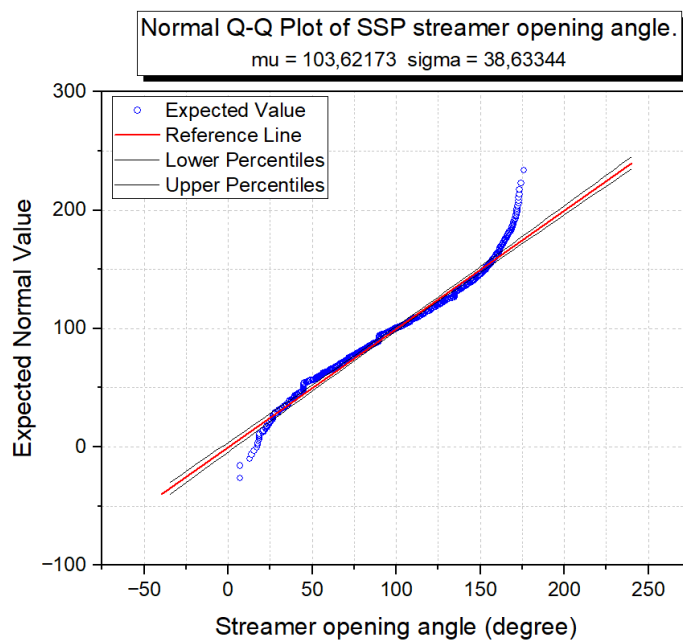


Figure A.4: QQ plot for the SSP configuration, indicating heavy tails. No normal distribution can be obtained from the data.

A.2 Linear leader propagation velocity

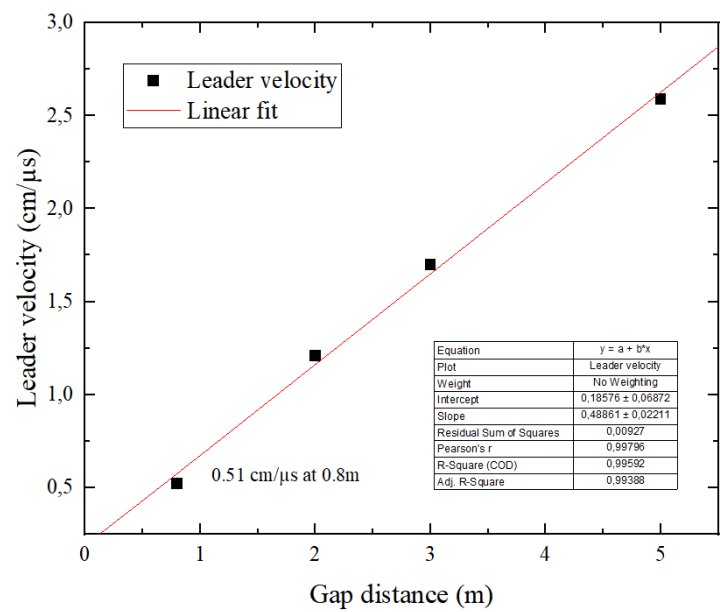


Figure A.5: Plot of leader velocities in rod to rod air gaps including the finding of this report. A linear relationship is found, shown by the linear fit in the data. Data points obtained from: [7]

A.3 Response Curve Phantom TMX 6410

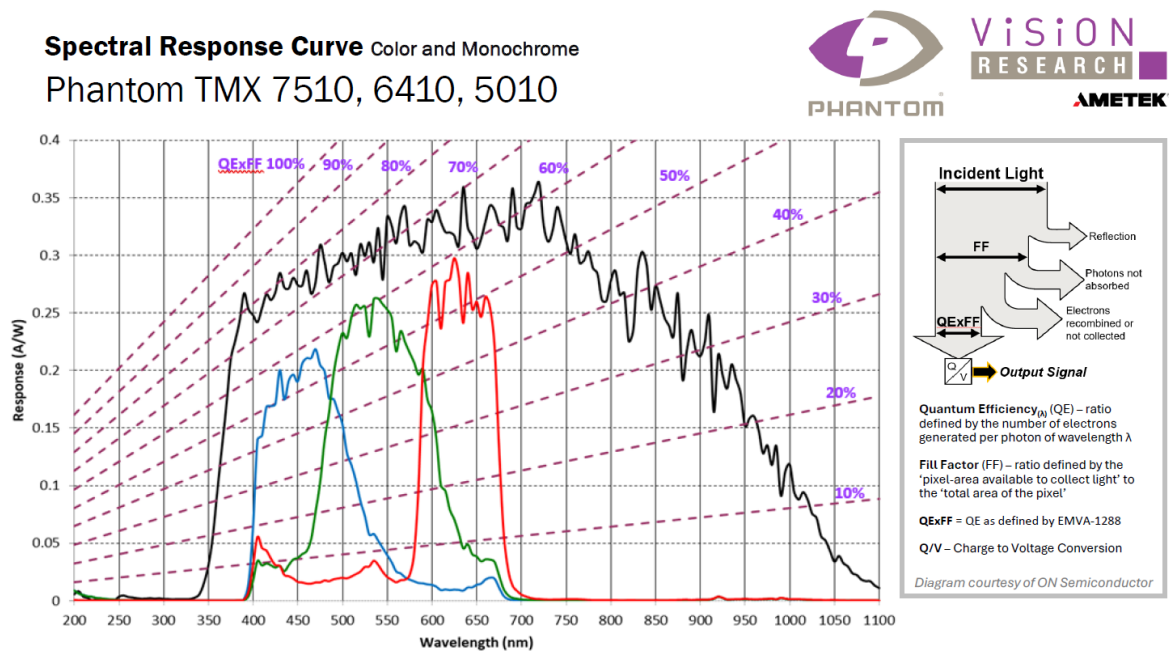


Figure A.6: Spectral response curve of the Phantom TMX 6410 high speed CMOS camera, in monochrome and color. Source: [6]